Cell Host & Microbe
Article

Inflammatory Monocytes Facilitate Adaptive CD4 T Cell Responses during Respiratory Fungal Infection

Tobias M. Hohl,[1,3,4,*] Amariliz Rivera,[1,3] Lauren Lipuma,[1] Alena Gallegos,[1] Chao Shi,[1] Mathias Mack,[2] and Eric G. Pamer[1,*]
[1]Infectious Disease Service, Department of Medicine, and Immunology Program, Sloan-Kettering Institute, Memorial Sloan-Kettering Cancer Center, New York, NY 10065, USA
[2]Department of Internal Medicine, University of Regensburg, 93053 Regensburg, Germany
[3]These authors contributed equally to this work
[4]Present address: Vaccine and Infectious Diseases Institute, Fred Hutchinson Cancer Research Center, Seattle, WA 98109, USA
*Correspondence: thohl@fhcrc.org (T.M.H.), pamere@mskcc.org (E.G.P.)
DOI 10.1016/j.chom.2009.10.007

SUMMARY

Aspergillus fumigatus, a ubiquitous fungus, causes invasive disease in immunocompromised humans. Although monocytes and antigen-specific CD4 T cells contribute to defense against inhaled fungal spores, how these cells interact during infection remains undefined. Investigating the role of inflammatory monocytes and monocyte-derived dendritic cells during fungal infection, we find that *A. fumigatus* infection induces an influx of chemokine receptor CCR2- and Ly6C-expressing inflammatory monocytes into lungs and draining lymph nodes. Depletion of CCR2$^+$ cells reduced *A. fumigatus* conidial transport from lungs to draining lymph nodes, abolished CD4 T cell priming following respiratory challenge, and impaired pulmonary fungal clearance. In contrast, depletion of CCR2$^+$Ly6C^{hi} monocytes during systemic fungal infection did not prevent CD4 T cell priming in the spleen. Our findings demonstrate that pulmonary CD4 T cell responses to inhaled spores require CCR2$^+$Ly6C^{hi} monocytes and their derivatives, revealing a compartmentally restricted function for these cells in adaptive respiratory immune responses.

INTRODUCTION

Inhalation of airborne fungal spores (conidia) is a daily event in mammalian life, and respiratory immune defenses provide effective and generally symptomless protection against invasive infection (Hohl and Feldmesser, 2007; Latge, 1999; Segal, 2009). *Aspergillus fumigatus* is a ubiquitous mold that, in immune compromised individuals, can cause invasive pulmonary infection leading to potentially lethal, disseminated disease. Though early defense against inhaled *A. fumigatus* spores is mediated by neutrophils (Bonnett et al., 2006; Gerson et al., 1984; Mehrad et al., 1999; Mircescu et al., 2009), protection against invasive disease in immunocompromised mice (Cenci et al., 1997, 2000) and humans (Hebart et al., 2002) also involves fungus-specific CD4 T cells. In immunocompromised patients, adoptive transfer of *A. fumigatus*-specific CD4 T cells can provide protection against invasive fungal infection (Beck et al., 2006; Perruccio et al., 2005).

Circulating monocytes have been implicated in defense against *A. fumigatus*, with evidence for direct killing of invasive fungal hyphae (Diamond et al., 1983; Roilides et al., 1994) and spores (Serbina et al., 2009a). *A. fumigatus* spores activate monocytes to express a broad range of cytokines, chemokines, and antimicrobial molecules (Cortez et al., 2006; Loeffler et al., 2009). TLR-mediated recognition of undefined fungal components and Dectin-1-mediated interactions with fungal β-glucans (Hohl et al., 2005) contribute to monocyte activation.

Monocytes are divided into subsets on the basis of chemokine receptor and Ly6C expression in mice and CD14 and CD16 expression in humans (Auffray et al., 2009b; Serbina et al., 2008). Murine Ly6C^{hi} monocytes are commonly referred to as inflammatory monocytes and express CCR2, a chemokine receptor that promotes emigration from the bone marrow (BM) into the circulation (Serbina and Pamer, 2006). *Ccr2*$^{-/-}$ mice have increased susceptibility to viral and microbial infections (Kurihara et al., 1997; Robben et al., 2005; Serbina et al., 2003), in large part due to retention of monocytes in the BM (Serbina and Pamer, 2006). *Ccr2*$^{-/-}$ mice also have decreased Th1 CD4 T cell responses (Nakano et al., 2009; Peters et al., 2000, 2001), a defect that has been correlated to impaired trafficking of monocytes to sites of infection and diminished transport of antigen to draining lymph nodes (Peters et al., 2000) or to decreased monocyte recruitment to inflamed lymph nodes and diminished production of IL-12 at the time of T cell priming (Nakano et al., 2009). In chronic fungal infection models, CCR2 deficiency appears to be associated with Th2 CD4 T cell differentiation (Blease et al., 2000; Traynor et al., 2000). Thus, although increasing evidence implicates monocytes in the activation and differentiation of CD4 T cell responses to viral (Aldridge et al., 2009; Nakano et al., 2009), mycobacterial (Peters et al., 2001), parasitic (Leon et al., 2007), and fungal infections (Traynor et al., 2000), it remains unclear whether monocytes are essential for these processes.

Although CCR2-mediated signals promote emigration of Ly6C^{hi} monocytes from the BM, the absence of CCR2 only reduces circulating monocyte levels by roughly 80% during homeostatic conditions (Serbina and Pamer, 2006). CCR2-independent

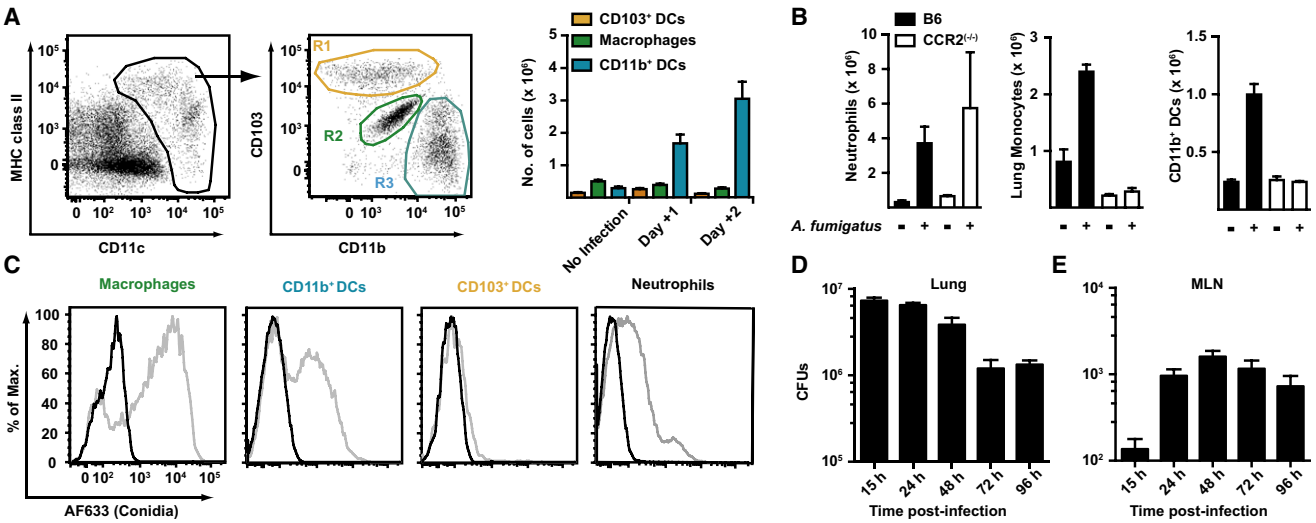

Figure 1. Inflammatory Cell Recruitment and Conidial MLN Transport during Respiratory Fungal Infection

(A) Gating strategy to define cell populations in the mouse lung. CD45$^+$CD11c$^+$MHC class II variable cells from naive C57BL/6 mice were classified as CD103$^+$ DCs (R1, yellow gate), autofluorescent CD11c$^+$ macrophages (R2, green gate), and CD11b$^+$ DCs (R3, blue gate) as in Sung et al. (2006).

(B and C) C57BL/6 mice (black bars) or *Ccr2*$^{-/-}$ mice (white bars) were infected with 1–2 × 10^7 conidia and euthanized at the indicated time points. Single-cell lung suspensions were enumerated and multiplied by the frequency of CD11b$^+$Ly6C$^+$Ly6G$^+$ neutrophils, CD11b$^+$Ly6C$^+$Ly6G$^-$ monocytes, or CD11b$^+$ DCs in the lung. The bar graphs in (B) show the average number (+ SEM) of the indicated cell populations. One of three representative experiments is shown with 3–4 mice per group. (C) The histograms depict the uptake of AF633-labeled conidia (gray lines) or unlabelled conidia (black lines) by the indicated lung cell subsets 2 days postinfection.

(D and E) C57BL/6 mice were infected with 1–2 × 10^7 conidia via the i.t. route, and CFUs in the (D) lungs and (E) MLN were determined at the indicated time points. The bar graphs show the average number (+ SEM) of CFUs per time point (n = 5/time point) from a representative experiment.

emigration of Ly6C^{hi} monocytes from the BM potentially confounds the interpretation of experiments using CCR2-deficient mice, given that peripheral tissues may be populated with sufficient numbers of monocytes and derivative cells in the steady state to obscure important phenotypes resulting from defective monocyte recruitment during infectious and inflammatory states. In addition, monocytes may employ CCR2-independent mechanisms to influence adaptive immune responses. Thus, an experimental system that targets monocytes and derivative cells for in vivo depletion would provide strong evidence regarding their role in triggering adaptive immune responses.

Herein, we have investigated the recruitment and activation of Ly6C^{hi} monocytes upon infection with *Aspergillus fumigatus* and, by generating a transgenic mouse strain that enables complete depletion of Ly6C^{hi} monocytes, determined that this cell population is essential for transport of fungal spores from the airways to draining lymph nodes. Whereas depletion of Ly6C^{hi} monocytes abrogates CD4 T cells' responses to respiratory challenge with fungal spores, systemic immune responses in the spleen are unaffected. Our studies reveal an essential, compartmentalized function for Ly6C^{hi} monocytes for the initiation of CD4 T cell responses following the inhalation of fungal spores.

RESULTS

Selective Expansion of Myeloid Cell Populations during Respiratory Fungal Infection

To characterize the pulmonary inflammatory cell influx following intratracheal (i.t.) *A. fumigatus* infection, we analyzed dissociated lung cells from naive mice by using flow cytometry to define distinct DC, macrophage, monocyte, and neutrophil populations in the steady state (Figure 1A). Lung leukocytes (CD45$^+$ cells) were analyzed for CD11c and MHC class II expression (Figure 1A), and CD11c$^+$ cells were divided into CD103$^+$ DCs (Figure 1A, R1, yellow gate), macrophages (Figure 1A, R2, green gate), or CD11b$^+$ DCs (Figure 1A, R3, blue gate) in accordance with published results (Sung et al., 2006). Following i.t. challenge with *A. fumigatus* conidia, rapid numeric expansion of CD11b$^+$ DCs, but not CD103$^+$ DCs or macrophages, was observed (Figure 1A). Neutrophil (defined as CD11b$^+$Ly6C$^+$Ly6G$^+$ cells) and monocyte (defined as CD11b$^+$Ly6C^{hi}Ly6G$^-$ cells) numbers increased substantially as well (Figure 1B). We next examined whether infection-induced changes in monocytes and derivative populations depends on intact CCR2 signaling. *Ccr2*$^{-/-}$ mice were infected and found to have diminished numbers of pulmonary monocytes and CD11b$^+$ DCs at 2 days postinfection (Figure 1B) compared to control mice. Loss of CCR2 signaling did not diminish pulmonary neutrophil influx (Figure 1B).

To define cell subsets that take up *A. fumigatus* conidia following i.t. inoculation and potentially contribute to CD4 T cell priming and differentiation, we infected mice with Alexa Fluor 633-labeled conidia and analyzed them at 2 days postinfection. Neutrophils and lung macrophages bound fluorescent conidia (Figure 1C), as anticipated from prior studies (reviewed in Latge, 1999). CD11b$^+$ DCs, a cell population that expands numerically during respiratory fungal infection, bound fluorescent conidia, but CD103$^+$ DCs, which do not increase in number following infection, did not bind labeled conidia in vivo.

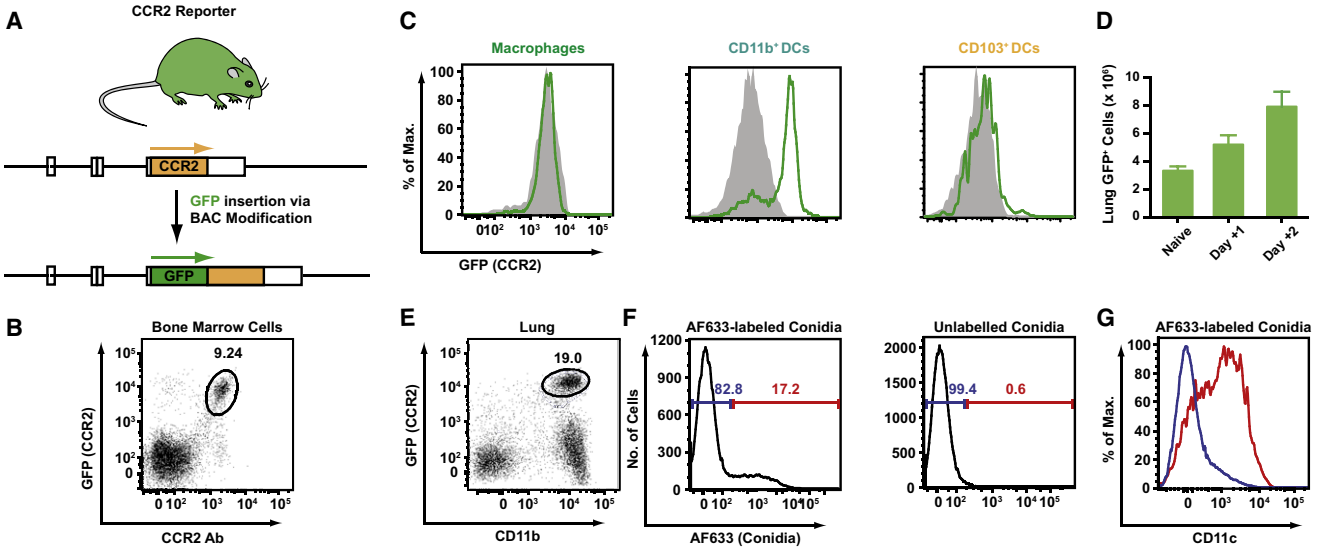

Figure 2. Characterization of CCR2 Reporter Mice

(A) Generation of CCR2 reporter mice. A BAC was modified to encode enhanced GFP under control of the murine CCR2 promoter. A stop codon was introduced at the 3′ transgene terminus followed by a single nucleotide deletion. Arrows indicate the expected translation products.

(B) The plot shows GFP expression and CCR2 Ab staining by CCR2 reporter BM cells.

(C) The histograms show GFP expression by lung DC subsets and macrophages isolated from naive CCR2 reporter (green lines) or nontransgenic C57BL/6 littermates (solid gray histograms).

(D) The bar graphs show the number (+ SEM) of lung GFP$^+$ cells in CCR2 reporter mice (n = 5/group) at the indicated time points postinfection.

(E–G) The plot in (E) shows CD11b expression by GFP$^+$ lung cells in day +2-infected CCR2 reporter mice (black gate). Lung GFP$^+$CD11b$^+$ cells (A, blue gate) were examined for uptake of AF633-labeled (F, left histogram) or unlabeled (F, right histogram) conidia. The blue and red gates indicate the frequency of AF633$^-$ and AF633$^+$ cells in each histogram, respectively. (G) CD11c expression by AF633$^-$ (blue line) and AF633$^+$ (red line) cell subsets among lung GFP$^+$CD11b$^+$ cells isolated from infected CCR2 reporter mice.

Kinetics of Conidial Transport to the MLN

The priming of *A. fumigatus*-specific CD4 T cells in the lung-draining mediastinal lymph node (MLN) can be observed as early as 4 days postinfection (Rivera et al., 2006). To determine the kinetics of conidial transport to the draining MLN, C57BL/6 mice were infected with 1–2 × 10^7 conidia, and the number of MLN CFUs was quantified at specified time points postinfection. At 15 hr postinfection, ~10^2 CFUs were cultured from the MLN (Figure 1D), and this number increased to ~10^3 CFUs by 48 hr postinfection, with a slight decline during the ensuing 48 hr. Pulmonary CFUs declined at each time point examined, with a nearly 10-fold drop between the 15 hr and 96 hr time points (Figure 4B). Thus, MLN conidial transport is rapid and peaks in the first 2 days postinfection, temporally coincident with the large pulmonary influx of monocytes and CD11b$^+$ DCs.

Development and Validation of CCR2 Reporter Mice

Because CD11b$^+$ DCs take up conidia and accumulate in a CCR2-dependent manner during respiratory fungal infection, a CCR2 reporter mouse was generated to track CCR2$^+$Ly6C^{hi} monocytes and their relationship to CD11b$^+$ lung DCs. A bacterial artificial chromosome encoding the murine CCR2 locus was modified to place GFP under control of the endogenous CCR2 promoter and incorporated into the germline of C57BL/6 mice (Figure 2B; for details, see methods in Serbina et al., 2009b). In CCR2 reporter mice, surface staining with a CCR2-specific monoclonal antibody (Mack et al., 2001) and transgenic expression of GFP correlate closely in BM cells (Figure 2B). GFP expression is high on circulating Ly6C^{hi} monocytes and diminished on Ly6C^{lo} monocytes (Figure S1 available online); these monocyte subsets express high and low levels of CCR2, respectively (Geissmann et al., 2003).

Although recent studies have shown that CD11b$^+$ and CD103$^+$ DCs both express CCR2 (Jakubzick et al., 2008b), characterization of naive CCR2 reporter mice revealed that CD11b$^+$ DCs express higher levels of the GFP transgene compared to CD103$^+$ DCs in the lung (Figure 2C). GFP transgene expression was not detected on neutrophils (data not shown) or autofluorescent lung CD11c$^+$ macrophages from CCR2 reporter mice by flow cytometric analysis.

Monocytes Differentiate into CD11b$^+$ Lung DCs during Respiratory Fungal Infection

During respiratory fungal infection, the number of GFP$^+$ cells in the lungs of CCR2 reporter mice nearly triples in the first 2 days postinfection (Figure 2D), and virtually all GFP$^+$ cells express CD11b$^+$ (Figure 2E). Approximately 15%–20% of CD11b$^+$GFP$^+$ cells contain fluorescent conidia (Figure 2F, left, red gate); this subset expresses high levels of CD11c (Figure 2G, red line) and MHC class II (data not shown), whereas GFP$^+$ cells that did not contain fluorescent conidia (Figure 2F, left, blue gate) express little or no CD11c. This result suggests that monocytes rapidly convert to CD11b$^+$ DCs upon or prior to conidial uptake.

Adoptive transfer experiments were performed to examine monocyte differentiation during respiratory fungal infection. CD45.1$^+$CD45.2$^+$ BM monocytes from CCR2 reporter mice

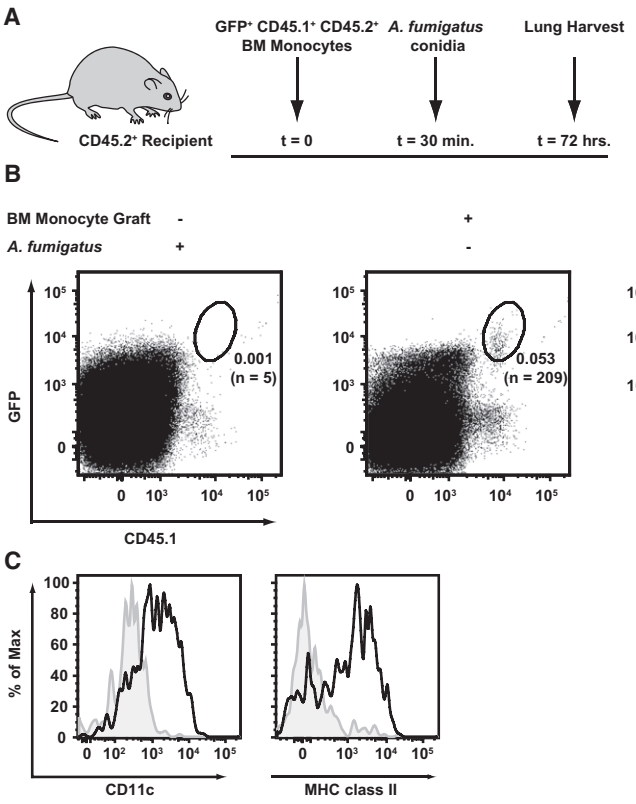

Figure 3. Bone Marrow Monocytes Differentiate into Lung CD11b$^+$ DCs during Respiratory Fungal Infection

(A) Overview of experimental scheme. Recipient CD45.2$^+$ mice received 8 × 10^5 flow-sorted CD45.1$^+$CD11c$^-$CD19$^-$Thy1.2$^-$NK1.1$^-$Ter119$^-$ GFP$^+$ BM cells from CCR2 reporter mice prior to infection.

(B) Representative plots of single-cell lung suspensions from *A. fumigatus*-infected (left, right) or uninfected mice (middle) that received BM monocytes (middle, right) or no graft (left). The plots are gated on CD45.2$^+$ cells (from 10^6 total recorded lung cells), and the frequency of CD45.1$^+$GFP$^+$ cells and the number of events in each gate is indicated.

(C) The histograms depict CD11c and MHC class II expression by gated CD45.1$^+$GFP$^+$ cells from infected (black line) or uninfected mice (filled gray histogram).

were purified on the basis of GFP expression and transferred into CD45.2$^+$ C57BL/6 recipient mice (Figure 3A). One-half of the recipient mice were infected with *A. fumigatus* 30 min later. The lungs of all experimental groups were harvested 3 days postinfection and analyzed by flow cytometry. CD45.1$^+$GFP$^+$ cells were found in the lungs of naive and infected recipient mice (Figure 3B), though the frequency and number of CD45.1$^+$GFP$^+$cells were higher in infected mice than in naive mice by a factor of ~2 and ~3, respectively. In infected mice, CD45.1$^+$GFP$^+$ cells in the lung express high levels of CD11c and MHC class II, whereas transferred CD45.1$^+$GFP$^+$ cells recovered from the lungs of naive mice (Figure 3C) express marginal levels of CD11c and MHC class II, consistent with the CD11b$^+$Ly6C$^+$Ly6G$^-$ flow cytometric phenotype of lung monocytes. Thus, the inflammatory response to respiratory fungal infection promotes monocyte differentiation into CD11b$^+$ lung DCs that are associated with conidial uptake. We did not observe CD45.1$^+$GFP$^+$ cells in the CD103$^+$ DC or macrophage gate in plots of stained lung cells from recipient mice (data not shown).

CD11b$^+$ Lung DCs Transport Conidia to the Draining MLN

To examine whether GFP$^+$ cells are associated with conidia in the MLN, we analyzed the MLN cell composition in CCR2 reporter mice at 48 hr postinfection, which corresponds to the peak in MLN *A. fumigatus* CFUs. At this time point, 2–3 × 10^4 GFP$^+$CD11b$^+$ cells accumulated in the MLN of infected (Figures 4A and 4B), but not naïve, mice. The majority of MLN GFP$^+$CD11b$^+$ cells express CD11c (Figure 4C, red gate) with a minor CD11c$^-$ population (Figure 4C, blue gate). MLN GFP$^+$CD11b$^+$CD11c$^+$ cells express high levels of MHC class II and CD86 (Figure 4D), whereas GFP$^+$CD11b$^+$CD11c$^-$ cells do not. Thus, on the basis of flow cytometric characterization, MLN GFP$^+$ CD11b$^+$CD11c$^+$ cells closely resemble lung CD11b$^+$ DCs.

Because CD11b$^+$ DCs take up conidia in the lung, we expected to find fluorescent conidia in the corresponding MLN GFP$^+$CD11b$^+$CD11c$^+$ cell population. Following infection with AF633-labeled conidia, ~5% of MLN GFP$^+$CD11b$^+$CD11c$^+$ cells bound fluorescent conidia (Figure 4E, left), whereas GFP$^+$CD11b$^+$CD11c$^-$ cells did not (Figure 4E, right), suggesting that monocyte-derived CD11b$^+$ lung DCs transport conidia to the MLN.

GFP$^+$CD11b$^+$ cells were sorted from the MLN of infected mice 48 hr postinfection and cultured ex vivo with naive, *A. fumigatus*-specific Af3.16 CD4 T cells (Rivera et al., 2006) in the presence of exogenously added Aspergillus antigens. Under these conditions, GFP$^+$CD11b$^+$ cells stimulated the proliferation of Af3.16 CD4 T cells, measured by tritiated thymidine incorporation (Figure 4F) and IL-2 release (data not shown), as efficiently as CD11c$^+$ splenic DCs purified from mice injected with Flt3L-secreting tumor cells. These results demonstrate that GFP$^+$CD11b$^+$ MLN cells isolated from *A. fumigatus*-infected mice have the capacity to prime naive fungus-specific CD4 T cells ex vivo.

Development, Validation, and Characterization of CCR2 Depleter Mice

To determine whether monocytes and derivative cells actively transport conidia to the MLN and to analyze their role in CD4 T cell priming, we generated a CCR2 depleter mouse using the diphtheria toxin (DT)-induced cell ablation strategy (Saito et al., 2001). The BAC clone RP23-182D4 was modified to encode a simian DT receptor (DTR) and enhanced cyan fluorescent protein (CFP). The DTR and CFP modules were separated by a linker sequence that contains an aphthovirus 2A cleavage site and was optimized for fluorescence (Figures 5A and S2).

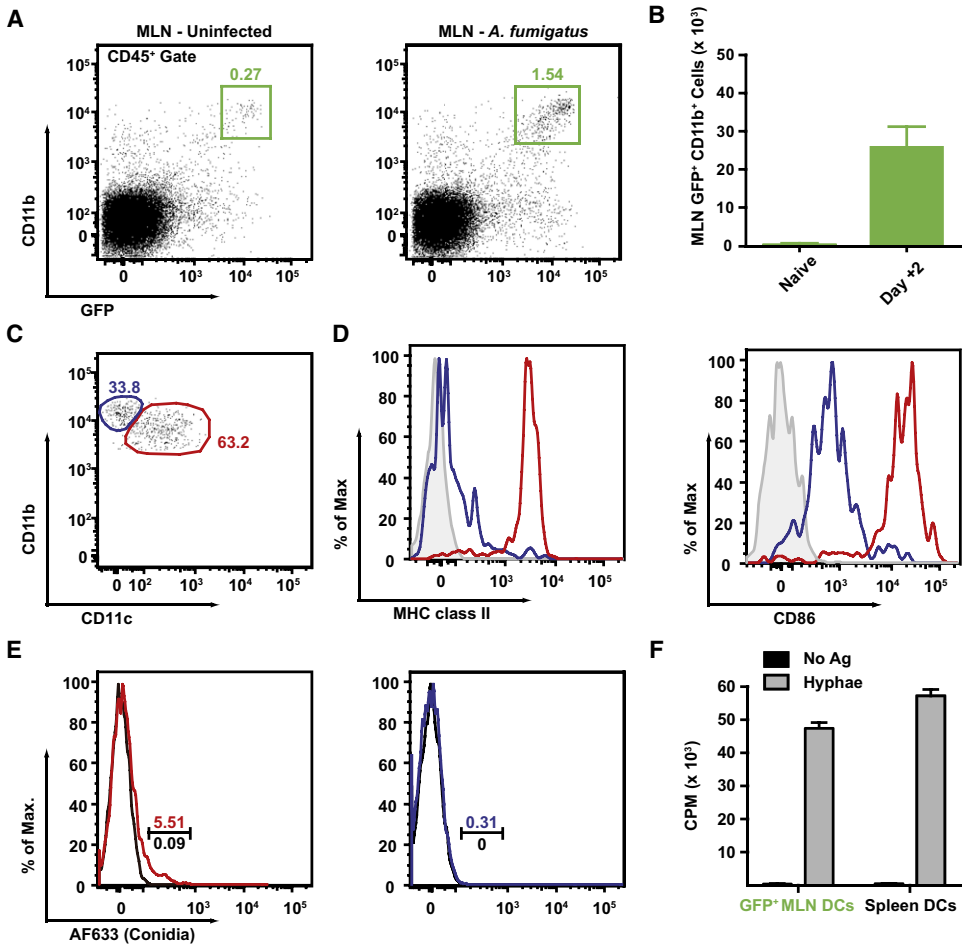

Figure 4. Influx of GFP$^+$CD11b$^+$ DCs in the MLN during Respiratory Fungal Infection

(A–D) GFP$^+$CD11b$^+$ cells accumulate in the MLN of *A. fumigatus*-infected mice. The plots in (A) and the bar graph in (B) show the frequency (A) and average number (+ SEM) (B) of MLN GFP$^+$CD11b$^+$ cells in infected (day +2) or naive CCR2 reporter mice. (C) MLN GFP$^+$CD11b$^+$ cells isolated from infected mice can be divided into two subsets on the basis of CD11c expression (blue and red gates). (D) The histograms show MHC class II and CD86 expression by the CD11c$^+$ (red line) or CD11c$^-$ subset of MLN GFP$^+$CD11b$^+$ cells (blue line). Isotype control staining is shown in the gray histograms. One of three (A and B) or two (C and D) experiments with 3–4 mice per group is shown.

(E) GFP$^+$CD11b$^+$ DCs are associated with fluorescent conidia. CCR2 reporter mice were infected with AF633-labeled (colored lines) or unlabeled conidia (black lines). MLN GFP$^+$CD11b$^+$ cells were divided into CD11c$^+$ DCs (red lines) or CD11c$^-$ monocytes (blue lines) and analyzed for AF633 fluorescence. The gate indicates the frequency of AF633$^+$ cells.

(F) MLN GFP$^+$CD11b$^+$ cells can prime naive Ag-specific CD4 T cells. 3.5 × 10^4 flow-sorted MLN GFP$^+$CD11b$^+$ cells harvested from infected CCR2 reporter mice or 5 × 10^4 MACS-enriched CD11c$^+$ DCs from Flt3L-treated mice were cultured for 48 hr with 5 × 10^4 Af3.16 CD4 T cells with (gray bars) or without (black bars) hyphal antigens prior to assessment of CD4 T cell proliferation by [^{3}H]-thymidine incorporation.

Two candidate founder mice were derived following oocyte injections, and a single CCR2 depleter founder line was expanded.

CFP expression in CCR2 depleter BM cells corresponds closely to CCR2 Ab staining (Figure S3A). Similar to CCR2 reporter mice, BM Ly6C^{hi} monocytes from CCR2 depleter mice uniformly express high levels of the fluorescent transgene (Figure S3B) and stain for the simian DTR transgene using an anti-human DTR Ab (Figure S3C). Circulating Ly6C^{hi} and Ly6C^{lo} monocytes express high levels and low levels of CFP, respectively (Figure S3D). CCR2 depleter mice were crossed to transgenic mice carrying a GFP transgene at the CX_3CR_1 locus (Jung et al., 2000). In progeny that contain both reporter genes, GFP^{lo}CFP^{hi} monocytes (Figure 6B, orange gate) correspond to Ly6C^{hi}CX$_3$CR$_1$^{lo}CCR2^{hi} monocytes. Conversely, GFP^{hi}CFP^{lo} monocytes (Figure 6B, purple gate) correspond to Ly6C^{lo}CX$_3$CR$_1$^{hi}CCR2^{lo} monocytes. Thus, the major circulating monocyte subsets can be distinguished on the basis of transgene expression.

CCR2 depleter mice were injected with a single 10 ng/g body weight dose of DT. No overt toxicity was observed, and DT-treated mice did not succumb during a 10 day observation period. Within 24 hr, > 99% of circulating monocytes were ablated, with recovery incipient at 48–72 hr following DT administration (Figure 6C). The blood monocyte frequency reached pretreatment levels by day +4, with a further increase evident

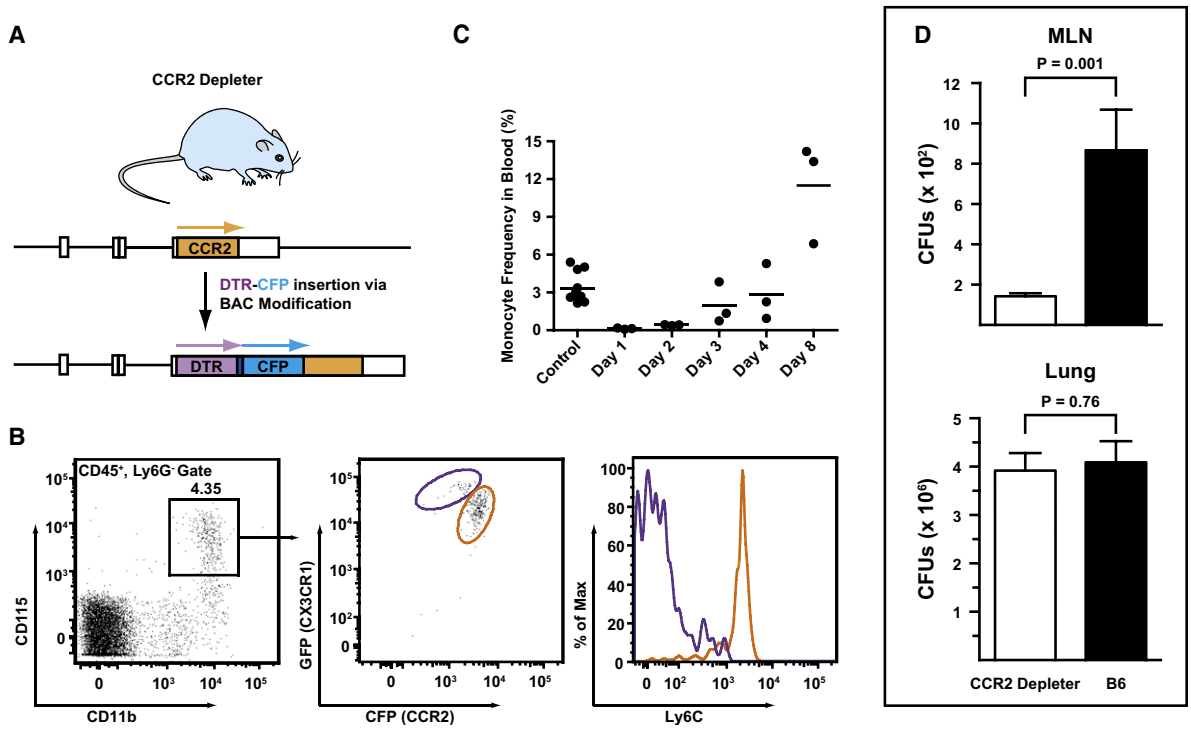

Figure 5. Abrogation of Conidial MLN Transport in CCR2 Depleter Mice

(A) Generation of CCR2 depleter mice. The BAC clone RP23-182D4 was modified to encode a simian DTR followed by a -$(GSG)_3$GTG- linker, a 19 residue aphthovirus 2A cleavage site (-APVKQTLNFDLLKLAGDVESNPGP-) (Donnelly et al., 2001), and enhanced CFP under control of the CCR2 promoter. A stop codon was introduced at the 3′ transgene terminus followed by a single nucleotide deletion. Arrows indicate the expected translation products.

(B and C) Transgene expression by monocytes and sensitivity to DT. Transgene expression by monocytes and ablation by DT administration. (B) $CD115^+$ blood monocytes (black gate, left) from $CX_3CR_1^{(gfp/+)}$ CCR2 depleter mice were analyzed for CFP, GFP, and Ly6C expression. In the left panel, the purple and orange gates indicate $GFP^{hi}CFP^{lo}$ and $GFP^{lo}CFP^{hi}$ monocytes, respectively. Ly6C expression by both subsets is shown in the histogram on the right. (C) CCR2 depleter mice were treated were 10 ng/g body weight DT via the i.p. route. The graph shows the percentage of $CD115^+$ monocytes among $CD45^+$ blood leukocytes at the indicate time points after DT treatment. Control mice include CCR2 depleter mice that did not receive DT and DT-treated nontransgenic littermates. One of two (B) or three (C) representative experiments is shown.

(D) CCR2 depleter mice (black bars) or control C57BL/6 mice (white bars) were treated with DT on day −1 and infected with 1–2 × 10^7 conidia on day 0. The histograms show the number (+ SEM) of MLN and lung CFUs 48 hr postinfection (n = 12–13/group) from two pooled experiments.

at day +8 (Figure 5C) and a return to homeostatic levels by day +10 (data not shown).

Monocyte Depletion and MLN Antigen Transport

The finding that monocytes infiltrate the lungs of *A. fumigatus*-infected mice and differentiate into $CD11b^+$ DCs that contain bound conidia is consistent with a role in MLN antigen delivery. It remains unclear, however, whether conidial transport to the MLN depends on DC uptake. Cell ablation experiments were performed to establish whether monocytes and derivative cells not only have the capacity to transport antigen to the MLN, but also are essential for this process.

CCR2 depleter and nontransgenic control mice were treated with a single DT dose and infected 24 hr later. The mice were euthanized 48 hr postinfection, and CFUs were determined in the MLN and lungs (Figure 5D). MLN CFUs in DT-treated CCR2 depleter mice were 85% lower than in nontransgenic controls, whereas lung CFUs were statistically equivalent in both groups (Figure 5D). Taken together with the MLN characterization of infected CCR2 reporter mice, these data indicate that monocyte-derived $CD11b^+$ DCs represent the major transport mechanism for *A. fumigatus* from the lung to the MLN.

Differential Impact of DT Treatment on DC Populations in the Lung and Spleen

Further characterization of CCR2 depleter mice demonstrated that DT treatment led to a rapid depletion of BM $Ly6C^+$ monocytes, with > 99% depletion within 12 hr of administration (data not shown). Of interest, MDPs, defined as $CX_3CR_1^+CD117^+Lin^-$ BM cells (Fogg et al., 2006), underwent depletion as well, with an ~90% reduction 24 hr following DT administration (Figure S4A), consistent with low-level expression of the CFP transgene (Figure S4B). Because MDPs not only give rise to monocytes, but also to nonmonocytic DC precursors, this finding suggested that DT treatment may affect splenic DC populations.

DT-induced cell depletion was, therefore, examined in lung and spleen samples from CCR2 depleter mice. A single DT dose led to the rapid depletion (by 12 hr) of lung- and spleen-resident $CD11b^+Ly6G^-Ly6C^{hi}$ monocytes, with a 2 $\log_{10}$ reduction in number (Figures 6A and 6B). In the lung, $CD11b^+$ DCs and

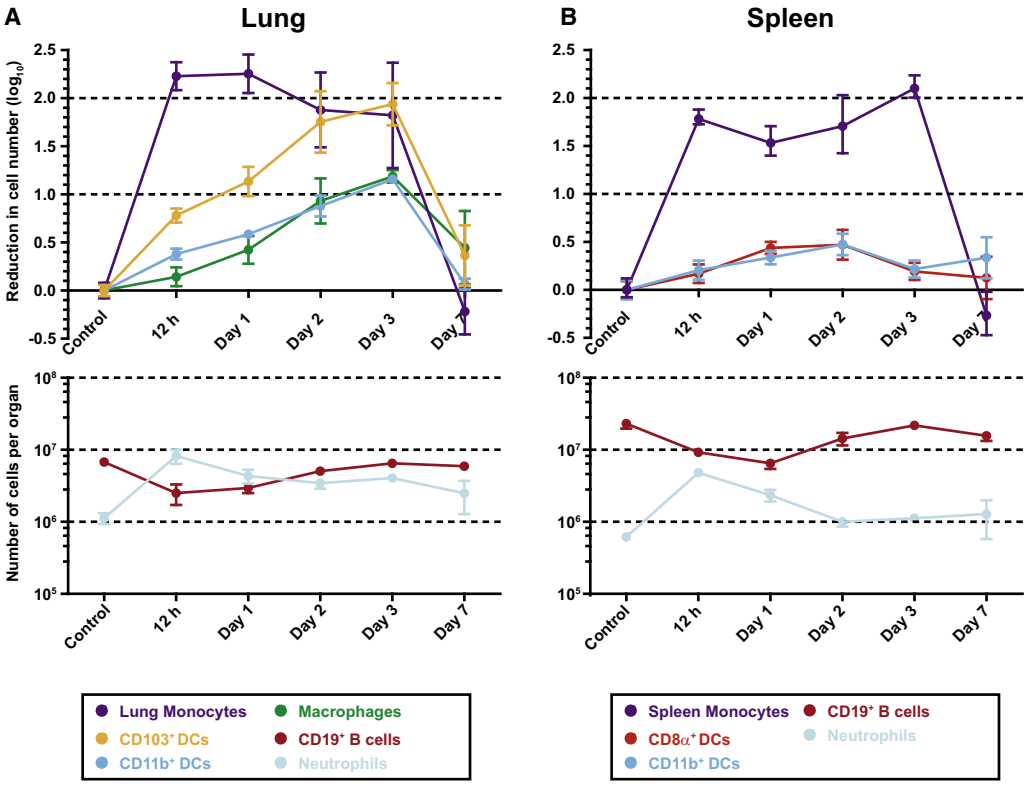

Figure 6. Depletion of Lung and Spleen DC Subsets in CCR2 Depleter Mice

(A and B) CCR2 depleter mice received no toxin (control) or 10 ng/g body weight DT at day 0. At the indicated time points, mice were euthanized, and single-cell suspensions from the lungs (A) and spleens (B) were enumerated and analyzed by flow cytometry to determine toxin-induced cell depletion. For the top panel in (A), the baseline lung monocyte, $CD103^+$ DC, $CD11b^+$ DC, and lung macrophage counts (± SEM) were (in log10 units) 6.167 ± 5.645, 5.401 ± 4.557, 5.786 ± 4.825, and 5.512 ± 4.781, respectively. For the top panel in (B), the baseline spleen monocyte, $CD8\alpha^+$ DC, and $CD11b^+$ DC counts (± SEM) were 5.746 ± 5.115, 4.978 ± 4.317, and 5.620 ± 4.916, respectively. One of three representative experiments is shown with 3–4 mice per group.

$CD103^+$ DCs underwent significant depletion (>1 $\log_{10}$ decease in number), albeit with slower kinetics. The maximal extent of cell depletion was evident on day +3 post-DT administration (Figure 6A). Similar results were observed for lung $CD11c^+$ macrophages. In contrast, the magnitude of DC depletion in the spleen was far less pronounced (Figure 6B). In three independent experiments, the number of $CD8\alpha^+CD11c^+$MHC class II^+ and $CD11b^+CD11c^+$MHC classII$^+$ DCs in the spleen underwent a modest reduction, typically by 0.2–0.4 $\log_{10}$ units (Figure 6B).

Lethally irradiated C57BL/6 mice were reconstituted with CCR2 depleter BM as a control to determine whether CCR2 expression on nonhematopoietic cells influences cell depletion in the lung and spleen. The extent and kinetics of DC depletion in the lung and spleen were similar in recipient mice reconstituted with CCR2 depleter BM cells (Figure S5). Thus, DT administration to CCR2 depleter mice selectively affects DCs in the lung, and $CD8\alpha^+$ and $CD11b^+$ DC subsets in the spleen are relatively unperturbed.

Monocyte Depletion and Impact on Antigen-Specific CD4 T Cell Responses

To determine whether the reduction in MLN antigen transport observed in CCR2 depleter mice affects antigen-specific CD4 T cell responses, we measured the proliferation, expansion, and trafficking of Af3.16 CD4 T cells in DT-treated CCR2 depleter mice 6 days postinfection. CCR2 depleter and nontransgenic C57BL/6 mice received 10^5 CFSE-labeled $CD90.1^+CD90.2^+$ Af3.16 CD4 T cells and DT on day −1 and day +1 postinfection, with 1–2 × 10^7 *A. fumigatus* conidia. The number and CFSE dilution profiles of transferred Af3.16 CD4 T cells were examined in the MLN, lung, and airways.

Af3.16 CD4 T cells underwent priming and expansion in the MLN of DT-treated control mice (Figures 7A and 7B). In contrast, the frequency of transgenic cells in the MLN CD4 gate was much lower in DT-treated CCR2 depleter mice, and little dilution of the CFSE label was observed (Figures 7A and 7B). Overall, Af3.16 CD4 T cells in the MLN of infected control mice underwent > 1000-fold expansion compared to naive mice, whereas only an ~10-fold expansion was observed in the MLN of infected CCR2 depleter mice. In sum, the number of Af3.16 CD4 T cells was ~100-fold greater both in the MLN and lungs of infected control mice compared to CCR2 depleter mice (Figure 7C), indicating that a major defect in the initiation of the CD4 T cell adaptive immune response is associated with the depletion of transgene-expressing cells.

The lung fungal burden was examined in the same group of mice to test whether the loss of *A. fumigatus*-specific CD4 T cell responses is associated with impaired fungal clearance.

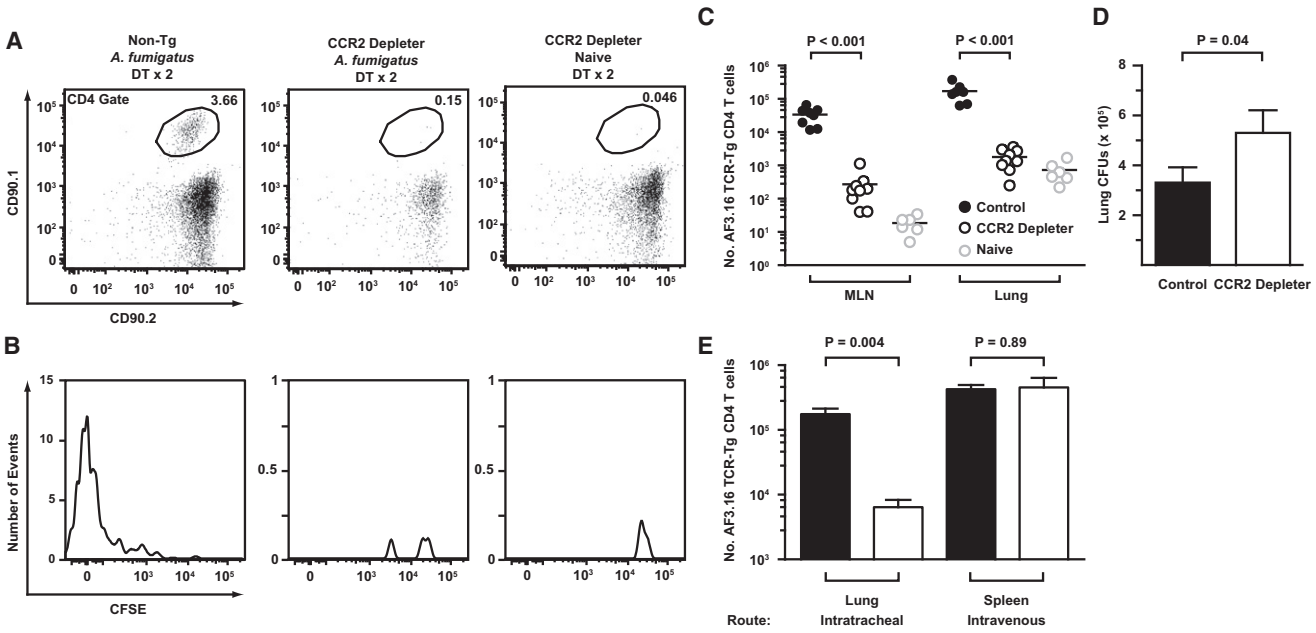

Figure 7. Depletion of CCR2$^+$ Cells Impairs CD4 T Cell Priming and Fungal Clearance in the Lung

(A–D) CCR2 depleter or nontransgenic littermates received 10^5 CFSE-labeled Af3.16 CD4 T cells on day −1, DT on day −1 and day +1, and 1–2 × 10^7 *A. fumigatus* conidia i.t. on day 0. The plots show representative examples of (A) the frequency of CD90.1$^+$CD90.2$^+$ Af3.16 TCR-Tg CD4 cells within the MLN CD4 gate and (B) the CFSE dilution profile of gated Af3.16 CD4 T cells. (C and D) The plots show (C) the number of MLN and lung Af3.16 CD4 T cells and (D) the average lung CFUs (± SEM) from DT-treated infected control (black circles or bar; n = 9), DT-treated infected CCR2 depleter (white circles or bar; n = 8), or DT-treated uninfected mice (gray circles; n = 6) 6 days postinfection from two pooled experiments.

(E) CCR2 depleter mice were treated with no DT (black bars) or one dose of DT (white bars) on day −1 and infected with *A. fumigatus* via the i.t. or i.v. route (day 0). The graph shows the average number of Af3.16 CD4 T cells (± SEM) in the lung and spleen 6 days postinfection.

In contrast to the day +2 time point (Figure 5D), CCR2 depleter mice had higher lung fungal burdens than control mice on day +6 postinfection (Figure 7D), consistent with the notion that CD4 T cell-dependent responses contribute to optimal antifungal defense. Thus, lung CD11b$^+$ DC-mediated conidial transport to the MLN is required for the priming and proliferation of antigen-specific CD4 T cells in the lung, and interruption of this process coincides with reduced *A. fumigatus* pulmonary clearance.

Although DT treatment led to depletion of lung CD11b$^+$ and CD103$^+$ DCs, splenic CD11b$^+$ and CD8α^+ DC subsets were relatively insensitive to DT. To examine the functional consequences of compartment-specific DC depletion, CCR2 depleter mice treated with a single dose of DT were infected via the i.t. or i.v. route, and the expansion of adoptively transferred Af3.16 TCR-Tg cells was measured in the lung and spleen, respectively. The number of splenic Af3.16 CD4 T cells was equivalent in CCR2 depleter and control mice infected via the i.v. route (Figure 7D), whereas the number of pulmonary Af3.16 CD4 T cells was severely reduced in CCR2 depleter mice compared to the control group infected via the i.t. route.

Similar results were observed in CCR2 depleter and control mice infected via the i.t. or i.v. route with an ActA$^-$ *Listeria monocytogenes* strain that expresses the *Mycobacterium tuberculosis* antigen ESAT-6. CCR2 depleter mice infected via the i.t. route showed a major defect in the number of lung ESAT-6-specific CD4 T cells (Gallegos et al., 2008), whereas CCR2 depleter mice infected via the i.v. route displayed normal expansion of splenic ESAT-6-specific CD4 T cells (Figure S6). These data demonstrate a compartment-specific role for monocyte-derived DCs in initiating adaptive immune responses to microbial pathogens.

DISCUSSION

Monocytes rapidly mobilize and rapidly differentiate in response to microbial challenges. Although monocytes are recruited to diverse host tissues and are implicated in innate and adaptive responses to viral and other microbial pathogens, their compartment-specific contributions to host defense remain incompletely defined. In part, our limited understanding of the role of monocytes in antimicrobial defense stems from the fact that selective in vivo depletion of monocytes has been difficult to achieve. Our results using a CCR2 depleter mouse strain demonstrate an essential role for monocytes in the priming and expansion of CD4 T cell responses following inhalation of a microbial pathogen. Loss of CD4 T cell priming following monocyte depletion correlates with a marked decrease in transport of fungal conidia to lung-draining MLNs and an ensuing defect in fungal clearance from the lung, thus implicating CCR2$^+$Ly6C^{hi} monocytes and derivative CD11b$^+$ DCs in this critical early step in the adaptive immune response.

We found that transferred BM monocytes rapidly differentiate in the presence of infection and express high levels of CD11c and MHC class II, giving rise to lung CD11b$^+$ DCs. Under these conditions, we did not observe monocyte differentiation into

$CD103^+$ DCs or pulmonary macrophages (data not shown). Furthermore, we did not observe CD11c and MHC class II upregulation upon transfer of cells into naive mice. It is likely that microbially induced inflammatory responses promote monocyte differentiation into $CD11b^+$ DCs with the capacity to take up and process microbial cargo at the portal of entry. $CD11b^+$ and $CD103^+$ lung DCs have been reported to discriminate between soluble and particulate forms of a model antigen, with uptake of the soluble form primarily by $CD11b^+$ DCs and the particulate form primarily by $CD103^+$ DCs (Jakubzick et al., 2008a). However, our results suggest that $CD11b^+$ DCs bind inhaled conidia, particles with an average diameter of 2–4 μm. In murine models of tuberculosis and leishmaniasis, $CD11b^+$ DCs take up fluorescent mycobacteria and parasites at infection sites and remain associated with the labeled microbes in the draining LNs (Leon et al., 2007; Wolf et al., 2007). Influenza virus nucleoprotein is found in the cytoplasm of migratory $CD11b^+$ and plasmacytoid DCs isolated from the lung-draining lymph nodes. (GeurtsvanKessel et al., 2008). An explanation for the differential uptake of microbial antigen by $CD103^-$ and $CD103^+$ DCs is the distinct complement of phagocytic receptors expressed by these DC subsets. Recent microarray analyses demonstrate that mRNA levels of receptors (e.g., dectin-1 and CD209) involved in conidial uptake are higher in $CD103^-$ than in $CD103^+$ DCs (del Rio et al., 2008; Serrano-Gomez et al., 2004). This difference may explain the in vivo difference in fungal cell uptake by $CD11b^+$ and $CD103^+$ lung DCs.

Much has been learned recently about the development of tissue DCs from precursors in the BM. Geissmann and colleagues identified a common macrophage and DC precursor (MDP) (Fogg et al., 2006) that gives rise to DC subsets both in lymphoid and nonlymphoid tissues. However, splenic conventional $CD8\alpha^-$ and $CD8\alpha^+$DCs (cDCs) develop in an Flt3L-dependent manner (Waskow et al., 2008) via a common DC precursor (CDP) in the BM and a pre-DC intermediate that can traffic from the BM to the spleen (Liu et al., 2007, 2009; Naik et al., 2006, 2007; Onai et al., 2007). Monocytes and descendent cells arise from MDPs as well (Auffray et al., 2009a; Fogg et al., 2006), albeit via a distinct developmental pathway (Liu et al., 2009). Recent studies using parabiosis, latex bead labeling, and adoptive transfer techniques found that circulating monocytes (Jakubzick et al., 2008b; Landsman and Jung, 2007; Landsman et al., 2007) have the capacity to give rise to lung DCs and macrophages in the steady state, with $CCR2^+Ly6C^{hi}$ monocytes preferentially giving rise to $CD103^+$ DCs and $Ly6C^{lo}$ monocytes preferentially giving rise to $CD11b^+$ DCs (Jakubzick et al., 2008b). It is clear that these steady-state pathways of monocyte differentiation are redirected during microbial infection (Serbina et al., 2008). For example, $Ly6C^{hi}$ monocytes infiltrating the spleens of *Listeria monocytogenes*-infected mice differentiate into TNF and iNOS-producing DCs (Tip-DCs) that are largely uninfected (Serbina et al., 2003). In contrast, in the setting of respiratory *A. fumigatus* infection, $Ly6C^{hi}$ monocytes differentiate into $CD11b^+$ DCs upon uptake of fungal conidia. This may explain differences in our study from results seen in the steady state (Jakubzick et al., 2008b).

The distinct developmental pathways of lung and splenic DCs likely contribute to the different degree of DC ablation noted in lung and splenic subsets in toxin-treated CCR2 depleter mice (Figure 6). Depletion of pulmonary $CD11b^+$ and $CD103^+$ DCs upon DT treatment of CCR2-DTR mice may result from depletion of monocyte precursors, but it is possible that tissue DC populations recently derived from monocytes continue to express DTR and thus are eliminated by toxin treatment. The delayed kinetics of lung DC subset depletion, however, suggests that monocyte loss is a more likely explanation for DC loss. Furthermore, the half-life of airway DCs is short. Holt and colleagues estimated a turnover time of ~2 days based on BM chimera experiments (Holt et al., 1994). In addition, respiratory DCs undergo basal migration to secondary lymphoid tissues via afferent lymphatics (Legge and Braciale, 2003). It is thus likely that pulmonary DC subsets are sensitive to the levels of circulating precursor cells, particularly following microbial challenge or in inflammatory states.

The finding that splenic CD4 T cell responses remain intact whereas pulmonary CD4 T cell responses are impaired may appear surprising, given the observation that MDPs are targeted in CCR2 depleter mice following toxin administration. Though bromodeoxyuridine labeling experiments suggests that both splenic subsets have half-lives on the order of 1.5–3 days (Kamath et al., 2000), more recent data show that splenic DCs may undergo limited cell division in situ (Liu et al., 2007) and extend the half-life of lymphoid organ DCs to 5–7 days. This latter estimate may contribute to differences in depletion seen in our experiments, given DT-induced depletion of the common MDP precursor. Consistent with this view, we observed that splenic cDCs were completely depleted in CCR2 depleter mice if the DT injection schedule was extended to four injections over 8 days (data not shown).

How do CCR2-expressing monocytes influence T cell responses? In our experiments, we demonstrate that they are necessary to transport conidia to draining lymph nodes. Although we demonstrate that monocyte-derived $CD11b^+$ DCs prime naive T cells ex vivo, we cannot be certain that they are performing this function in vivo. Thus, the possibility remains that monocytes transport conidia to lymph nodes and then transfer antigen to lymph node-resident DCs. During influenza virus infection, this scenario appears highly likely for the priming of CD8 T cell responses by MLN resident $CD11b^-CD8\alpha^+$ DCs (Belz et al., 2004) or $CD11b^-CD8\alpha^-$ DCs and CD4 T cell responses by MLN $CD11b^-CD8\alpha^-$ DCs (GeurtsvanKessel et al., 2008), given that these subsets do not participate in viral antigen delivery to the MLN. The recent development of mice with defined genetic lesions in lymph node-resident $CD8\alpha^+$ DC development (Hildner et al., 2008) may provide a framework to address these questions in more detail.

Invasive aspergillosis (IA) is a disease of the highly immunocompromised host, occurring most commonly in patients undergoing allogeneic BM transplantation (Segal, 2009). Although neutropenia is a well-appreciated risk factor for invasive fungal infection, recent studies have demonstrated that human monocyte subsets can also directly inhibit germination of *A. fumigatus* conidia (Serbina et al., 2009a). Whether human or murine monocytes play a critical role for the success of vaccine strategies that target IA remains an important line of investigation. Preclinical studies have evaluated a large number of proteinaceous, lipidic, and carbohydrate antigens in combination with adjuvants or DCs as vaccine candidates (Bozza et al., 2009; Cenci et al., 2000;

Torosantucci et al., 2005, 2009). Our demonstration that selective depletion of monocytes in the setting of *A. fumigatus* infection abrogates pathogen-specific CD4 T cell responses suggests that temporary loss of monocytes in clinical settings has important implications for CD4 T cell-dependent vaccination strategies and the development of adaptive antifungal defenses.

EXPERIMENTAL PROCEDURES

Mice

C57BL/6, C57BL/6.SJL, *Ccr2*$^{-/-}$, $CX_3CR_1^{(gfp/gfp)}$ (purchased from Jackson Laboratories), Af3.16 TCR-Tg (Rivera et al., 2006), and ESAT-6 clone 7 TCR-Tg (Gallegos et al., 2008) mice were housed and bred at the MSKCC Research Animal Resource Center. The generation of CCR2 reporter and CCR2 depleter mice is described in Serbina et al. (2009b) and the Supplemental Experimental Procedures, respectively. All strains were generated on or backcrossed > 10 generations on the C57BL/6 background.

Chemicals and Reagents

Diphtheria toxin was obtained from List Biological Laboratories (Cat. No. 150), reconstituted at 1 mg/ml in PBS, and frozen at −80°C. Mice received 10 ng/g DT via the i.p. route in 0.2–0.3 ml PBS.

Aspergillus Growth and Storage

Mice were infected via the i.t. (1–2 × 10^7 conidia) or i.v. (10^5 conidia) route with *A. fumigatus* strain Af293. For fluorescent labeling, 1–2 × 10^8 conidia were incubated with 100 μg/ml Alexa Fluor 633 succinimidyl ester (Invitrogen) at 37°C for 1 hr according to manufacturer's instructions.

Adoptive Cell Transfer

For adoptive transfer of 10^5 Af3.16 CD4 T cells via lateral tail vein injection, CD4 T cells from the spleens and LNs of Af3.16 TCR-Tg mice were collected, labeled with 5 μM CFSE (Invitrogen) as indicated, and purified by MACS using CD4 microbeads (Miltenyi Biotech). For adoptive transfer of BM monocytes, single-cell BM suspensions from $CD45.1^+CD45.2^+CCR2$ reporter mice were stained with APC-linked anti-CD3, -CD11c, -CD19, -NK1.1, and -Ter119, and GFP^+APC^- cells were isolated by sorting on a MoFlo flow cytometer (Cytomation) and injected into recipient mice.

Flow Cytometry

Single-cell lung, spleen, BM, and lymph node suspensions were prepared. Lungs and spleens were minced in PBS, 5% FCS, 3 mg/ml collagenase type IV (Worthington), and 20 U/ml DNase (Roche) and were incubated at 37°C for 60 min and 15 min, respectively. Following RBC lysis, cell suspensions were enumerated using a Z2 Coulter counter (Beckman Instruments) with a 6–15 μm window, stained with antibodies listed in the Supplemental Experimental Procedures, and analyzed on a BD LSR II cytometer.

In Vitro T Cell Priming

GFP^+CD11b^+ DCs were sorted from the MLN of *A. fumigatus*-infected CCR2 reporter mice 2 days postinfection, and 3.5 × 10^4 cells were seeded per well in a 96-well plate in quadruplicate. MACS-purified $CD11c^+$ control DCs (5 × 10^4 per well) were harvested from the spleens of C57BL/6 mice injected with a B16-Flt3L tumor line. 5 × 10^4 Af3.16 CD4 T cells from *Rag-2*$^{-/-}$ donors were purified over anti-CD4 microbeads and added to each well containing APCs. *A. fumigatus* hyphal antigens were added at a 1:200 final dilution together with 1 μg/ml voriconazole (Pfizer). After 2 days, culture supernatant IL-2 levels were measured by ELISA. Fresh media and 1 μCi of ^{3}[H]-thymidine were added to the wells, and the samples were processed for liquid scintillation analysis 1 day later.

Statistical Comparisons

The unpaired Student's t test was used for statistical analysis using GraphPad Prism 5.0 software. $p < 0.05$ was considered statistically significant.

SUPPLEMENTAL DATA

Supplemental Data include Supplemental Experimental Procedures and six figures and can be found with this article online at http://www.cell.com/cell-host-microbe/supplemental/S1931-3128(09)00349-7.

ACKNOWLEDGMENTS

We thank Ingrid Leiner for outstanding technical support and Ting Jia, Alexander Lesokhin, and Natalya Serbina for helpful comments and suggestions. This work was supported by NIH grants K08 AI071998 to T.M.H., K01 CA117914-01A1 to A.R., F32 AI074248 to A.G., and R01 AI067359 and P01 CA-023766 to E.G.P.

Received: August 23, 2009
Revised: October 9, 2009
Accepted: October 22, 2009
Published: November 18, 2009

REFERENCES

Aldridge, J.R., Jr., Moseley, C.E., Boltz, D.A., Negovetich, N.J., Reynolds, C., Franks, J., Brown, S.A., Doherty, P.C., Webster, R.G., and Thomas, P.G. (2009). TNF/iNOS-producing dendritic cells are the necessary evil of lethal influenza virus infection. Proc. Natl. Acad. Sci. USA *106*, 5306–5311.

Auffray, C., Fogg, D.K., Narni-Mancinelli, E., Senechal, B., Trouillet, C., Saederup, N., Leemput, J., Bigot, K., Campisi, L., Abitbol, M., et al. (2009a). CX3CR1+ CD115+ CD135+ common macrophage/DC precursors and the role of CX3CR1 in their response to inflammation. J. Exp. Med. *206*, 595–606.

Auffray, C., Sieweke, M.H., and Geissmann, F. (2009b). Blood monocytes: development, heterogeneity, and relationship with dendritic cells. Annu. Rev. Immunol. *27*, 669–692.

Beck, O., Topp, M.S., Koehl, U., Roilides, E., Simitsopoulou, M., Hanisch, M., Sarfati, J., Latge, J.P., Klingebiel, T., Einsele, H., and Lehrnbecher, T. (2006). Generation of highly purified and functionally active human TH1 cells against Aspergillus fumigatus. Blood *107*, 2562–2569.

Belz, G.T., Smith, C.M., Kleinert, L., Reading, P., Brooks, A., Shortman, K., Carbone, F.R., and Heath, W.R. (2004). Distinct migrating and nonmigrating dendritic cell populations are involved in MHC class I-restricted antigen presentation after lung infection with virus. Proc. Natl. Acad. Sci. USA *101*, 8670–8675.

Blease, K., Mehrad, B., Standiford, T.J., Lukacs, N.W., Gosling, J., Boring, L., Charo, I.F., Kunkel, S.L., and Hogaboam, C.M. (2000). Enhanced pulmonary allergic responses to Aspergillus in CCR2−/− mice. J. Immunol. *165*, 2603–2611.

Bonnett, C.R., Cornish, E.J., Harmsen, A.G., and Burritt, J.B. (2006). Early neutrophil recruitment and aggregation in the murine lung inhibit germination of Aspergillus fumigatus Conidia. Infect. Immun. *74*, 6528–6539.

Bozza, S., Clavaud, C., Giovannini, G., Fontaine, T., Beauvais, A., Sarfati, J., D'Angelo, C., Perruccio, K., Bonifazi, P., Zagarella, S., et al. (2009). Immune sensing of Aspergillus fumigatus proteins, glycolipids, and polysaccharides and the impact on Th immunity and vaccination. J. Immunol. *183*, 2407–2414.

Cenci, E., Perito, S., Enssle, K.H., Mosci, P., Latge, J.P., Romani, L., and Bistoni, F. (1997). Th1 and Th2 cytokines in mice with invasive aspergillosis. Infect. Immun. *65*, 564–570.

Cenci, E., Mencacci, A., Bacci, A., Bistoni, F., Kurup, V.P., and Romani, L. (2000). T cell vaccination in mice with invasive pulmonary aspergillosis. J. Immunol. *165*, 381–388.

Cortez, K.J., Lyman, C.A., Kottilil, S., Kim, H.S., Roilides, E., Yang, J., Fullmer, B., Lempicki, R., and Walsh, T.J. (2006). Functional genomics of innate host defense molecules in normal human monocytes in response to Aspergillus fumigatus. Infect. Immun. *74*, 2353–2365.

del Rio, M.L., Rodriguez-Barbosa, J.I., Bolter, J., Ballmaier, M., Dittrich-Breiholz, O., Kracht, M., Jung, S., and Forster, R. (2008). CX3CR1+ c-kit+ bone marrow cells give rise to CD103+ and CD103- dendritic cells with distinct functional properties. J. Immunol. *181*, 6178–6188.

Diamond, R.D., Huber, E., and Haudenschild, C.C. (1983). Mechanisms of destruction of Aspergillus fumigatus hyphae mediated by human monocytes. J. Infect. Dis. *147*, 474–483.

Donnelly, M.L., Hughes, L.E., Luke, G., Mendoza, H., ten Dam, E., Gani, D., and Ryan, M.D. (2001). The 'cleavage' activities of foot-and-mouth disease virus 2A site-directed mutants and naturally occurring '2A-like' sequences. J. Gen. Virol. *82*, 1027–1041.

Fogg, D.K., Sibon, C., Miled, C., Jung, S., Aucouturier, P., Littman, D.R., Cumano, A., and Geissmann, F. (2006). A clonogenic bone marrow progenitor specific for macrophages and dendritic cells. Science *311*, 83–87.

Gallegos, A.M., Pamer, E.G., and Glickman, M.S. (2008). Delayed protection by ESAT-6-specific effector CD4+ T cells after airborne M. tuberculosis infection. J. Exp. Med. *205*, 2359–2368.

Geissmann, F., Jung, S., and Littman, D.R. (2003). Blood monocytes consist of two principal subsets with distinct migratory properties. Immunity *19*, 71–82.

Gerson, S.L., Talbot, G.H., Hurwitz, S., Strom, B.L., Lusk, E.J., and Cassileth, P.A. (1984). Prolonged granulocytopenia: the major risk factor for invasive pulmonary aspergillosis in patients with acute leukemia. Ann. Intern. Med. *100*, 345–351.

GeurtsvanKessel, C.H., Willart, M.A., van Rijt, L.S., Muskens, F., Kool, M., Baas, C., Thielemans, K., Bennett, C., Clausen, B.E., Hoogsteden, H.C., et al. (2008). Clearance of influenza virus from the lung depends on migratory langerin+CD11b- but not plasmacytoid dendritic cells. J. Exp. Med. *205*, 1621–1634.

Hebart, H., Bollinger, C., Fisch, P., Sarfati, J., Meisner, C., Baur, M., Loeffler, J., Monod, M., Latge, J.P., and Einsele, H. (2002). Analysis of T-cell responses to Aspergillus fumigatus antigens in healthy individuals and patients with hematologic malignancies. Blood *100*, 4521–4528.

Hildner, K., Edelson, B.T., Purtha, W.E., Diamond, M., Matsushita, H., Kohyama, M., Calderon, B., Schraml, B.U., Unanue, E.R., Diamond, M.S., et al. (2008). Batf3 deficiency reveals a critical role for CD8alpha+ dendritic cells in cytotoxic T cell immunity. Science *322*, 1097–1100.

Hohl, T.M., and Feldmesser, M. (2007). Aspergillus fumigatus: principles of pathogenesis and host defense. Eukaryot. Cell *6*, 1953–1963.

Hohl, T.M., Van Epps, H.L., Rivera, A., Morgan, L.A., Chen, P.L., Feldmesser, M., and Pamer, E.G. (2005). Aspergillus fumigatus triggers inflammatory responses by stage-specific beta-glucan display. PLoS Pathog. *1*, e30.

Holt, P.G., Haining, S., Nelson, D.J., and Sedgwick, J.D. (1994). Origin and steady-state turnover of class II MHC-bearing dendritic cells in the epithelium of the conducting airways. J. Immunol. *153*, 256–261.

Jakubzick, C., Helft, J., Kaplan, T.J., and Randolph, G.J. (2008a). Optimization of methods to study pulmonary dendritic cell migration reveals distinct capacities of DC subsets to acquire soluble versus particulate antigen. J. Immunol. Methods *337*, 121–131.

Jakubzick, C., Tacke, F., Ginhoux, F., Wagers, A.J., van Rooijen, N., Mack, M., Merad, M., and Randolph, G.J. (2008b). Blood monocyte subsets differentially give rise to CD103+ and CD103- pulmonary dendritic cell populations. J. Immunol. *180*, 3019–3027.

Jung, S., Aliberti, J., Graemmel, P., Sunshine, M.J., Kreutzberg, G.W., Sher, A., and Littman, D.R. (2000). Analysis of fractalkine receptor CX(3)CR1 function by targeted deletion and green fluorescent protein reporter gene insertion. Mol. Cell. Biol. *20*, 4106–4114.

Kamath, A.T., Pooley, J., O'Keeffe, M.A., Vremec, D., Zhan, Y., Lew, A.M., D'Amico, A., Wu, L., Tough, D.F., and Shortman, K. (2000). The development, maturation, and turnover rate of mouse spleen dendritic cell populations. J. Immunol. *165*, 6762–6770.

Kurihara, T., Warr, G., Loy, J., and Bravo, R. (1997). Defects in macrophage recruitment and host defense in mice lacking the CCR2 chemokine receptor. J. Exp. Med. *186*, 1757–1762.

Landsman, L., and Jung, S. (2007). Lung macrophages serve as obligatory intermediate between blood monocytes and alveolar macrophages. J. Immunol. *179*, 3488–3494.

Landsman, L., Varol, C., and Jung, S. (2007). Distinct differentiation potential of blood monocyte subsets in the lung. J. Immunol. *178*, 2000–2007.

Latge, J.P. (1999). Aspergillus fumigatus and aspergillosis. Clin. Microbiol. Rev. *12*, 310–350.

Legge, K.L., and Braciale, T.J. (2003). Accelerated migration of respiratory dendritic cells to the regional lymph nodes is limited to the early phase of pulmonary infection. Immunity *18*, 265–277.

Leon, B., Lopez-Bravo, M., and Ardavin, C. (2007). Monocyte-derived dendritic cells formed at the infection site control the induction of protective T helper 1 responses against Leishmania. Immunity *26*, 519–531.

Liu, K., Victora, G.D., Schwickert, T.A., Guermonprez, P., Meredith, M.M., Yao, K., Chu, F.F., Randolph, G.J., Rudensky, A.Y., and Nussenzweig, M. (2009). In vivo analysis of dendritic cell development and homeostasis. Science *324*, 392–397.

Liu, K., Waskow, C., Liu, X., Yao, K., Hoh, J., and Nussenzweig, M. (2007). Origin of dendritic cells in peripheral lymphoid organs of mice. Nat. Immunol. *8*, 578–583.

Loeffler, J., Haddad, Z., Bonin, M., Romeike, N., Mezger, M., Schumacher, U., Kapp, M., Gebhardt, F., Grigoleit, G.U., Stevanovic, S., et al. (2009). Interaction analyses of human monocytes co-cultured with different forms of Aspergillus fumigatus. J. Med. Microbiol. *58*, 49–58.

Mack, M., Cihak, J., Simonis, C., Luckow, B., Proudfoot, A.E., Plachy, J., Bruhl, H., Frink, M., Anders, H.J., Vielhauer, V., et al. (2001). Expression and characterization of the chemokine receptors CCR2 and CCR5 in mice. J. Immunol. *166*, 4697–4704.

Mehrad, B., Strieter, R.M., Moore, T.A., Tsai, W.C., Lira, S.A., and Standiford, T.J. (1999). CXC chemokine receptor-2 ligands are necessary components of neutrophil-mediated host defense in invasive pulmonary aspergillosis. J. Immunol. *163*, 6086–6094.

Mircescu, M.M., Lipuma, L., van Rooijen, N., Pamer, E.G., and Hohl, T.M. (2009). Essential Role for Neutrophils but not Alveolar Macrophages at Early Time Points following Aspergillus fumigatus Infection. J. Infect. Dis. *200*, 647–656.

Naik, S.H., Metcalf, D., van Nieuwenhuijze, A., Wicks, I., Wu, L., O'Keeffe, M., and Shortman, K. (2006). Intrasplenic steady-state dendritic cell precursors that are distinct from monocytes. Nat. Immunol. *7*, 663–671.

Naik, S.H., Sathe, P., Park, H.Y., Metcalf, D., Proietto, A.I., Dakic, A., Carotta, S., O'Keeffe, M., Bahlo, M., Papenfuss, A., et al. (2007). Development of plasmacytoid and conventional dendritic cell subtypes from single precursor cells derived in vitro and in vivo. Nat. Immunol. *8*, 1217–1226.

Nakano, H., Lin, K.L., Yanagita, M., Charbonneau, C., Cook, D.N., Kakiuchi, T., and Gunn, M.D. (2009). Blood-derived inflammatory dendritic cells in lymph nodes stimulate acute T helper type 1 immune responses. Nat. Immunol. *10*, 394–402.

Onai, N., Obata-Onai, A., Schmid, M.A., Ohteki, T., Jarrossay, D., and Manz, M.G. (2007). Identification of clonogenic common Flt3+M-CSFR+ plasmacytoid and conventional dendritic cell progenitors in mouse bone marrow. Nat. Immunol. *8*, 1207–1216.

Perruccio, K., Tosti, A., Burchielli, E., Topini, F., Ruggeri, L., Carotti, A., Capanni, M., Urbani, E., Mancusi, A., Aversa, F., et al. (2005). Transferring functional immune responses to pathogens after haploidentical hematopoietic transplantation. Blood *106*, 4397–4406.

Peters, W., Dupuis, M., and Charo, I.F. (2000). A mechanism for the impaired IFN-gamma production in C-C chemokine receptor 2 (CCR2) knockout mice: role of CCR2 in linking the innate and adaptive immune responses. J. Immunol. *165*, 7072–7077.

Peters, W., Scott, H.M., Chambers, H.F., Flynn, J.L., Charo, I.F., and Ernst, J.D. (2001). Chemokine receptor 2 serves an early and essential role in resistance to Mycobacterium tuberculosis. Proc. Natl. Acad. Sci. USA *98*, 7958–7963.

Rivera, A., Ro, G., Van Epps, H.L., Simpson, T., Leiner, I., Sant'Angelo, D.B., and Pamer, E.G. (2006). Innate immune activation and CD4+ T cell priming during respiratory fungal infection. Immunity *25*, 665–675.

Robben, P.M., LaRegina, M., Kuziel, W.A., and Sibley, L.D. (2005). Recruitment of Gr-1+ monocytes is essential for control of acute toxoplasmosis. J. Exp. Med. *201*, 1761–1769.

Roilides, E., Holmes, A., Blake, C., Venzon, D., Pizzo, P.A., and Walsh, T.J. (1994). Antifungal activity of elutriated human monocytes against Aspergillus fumigatus hyphae: enhancement by granulocyte-macrophage colony-stimulating factor and interferon-gamma. J. Infect. Dis. *170*, 894–899.

Saito, M., Iwawaki, T., Taya, C., Yonekawa, H., Noda, M., Inui, Y., Mekada, E., Kimata, Y., Tsuru, A., and Kohno, K. (2001). Diphtheria toxin receptor-mediated conditional and targeted cell ablation in transgenic mice. Nat. Biotechnol. *19*, 746–750.

Segal, B.H. (2009). Aspergillosis. N. Engl. J. Med. *360*, 1870–1884.

Serbina, N.V., Salazar-Mather, T.P., Biron, C.A., Kuziel, W.A., and Pamer, E.G. (2003). TNF/iNOS-producing dendritic cells mediate innate immune defense against bacterial infection. Immunity *19*, 59–70.

Serbina, N.V., and Pamer, E.G. (2006). Monocyte emigration from bone marrow during bacterial infection requires signals mediated by chemokine receptor CCR2. Nat. Immunol. *7*, 311–317.

Serbina, N.V., Jia, T., Hohl, T.M., and Pamer, E.G. (2008). Monocyte-mediated defense against microbial pathogens. Annu. Rev. Immunol. *26*, 421–452.

Serbina, N.V., Cherny, M., Shi, C., Bleau, S.A., Collins, N.H., Young, J.W., and Pamer, E.G. (2009a). Distinct responses of human monocyte subsets to Aspergillus fumigatus conidia. J. Immunol. *183*, 2678–2687.

Serbina, N.V., Hohl, T.M., Cherny, M., and Pamer, E.G. (2009b). Selective expansion of the monocytic lineage directed by bacterial infection. J. Immunol. *183*, 1900–1910.

Serrano-Gomez, D., Dominguez-Soto, A., Ancochea, J., Jimenez-Heffernan, J.A., Leal, J.A., and Corbi, A.L. (2004). Dendritic cell-specific intercellular adhesion molecule 3-grabbing nonintegrin mediates binding and internalization of Aspergillus fumigatus conidia by dendritic cells and macrophages. J. Immunol. *173*, 5635–5643.

Sung, S.S., Fu, S.M., Rose, C.E., Jr., Gaskin, F., Ju, S.T., and Beaty, S.R. (2006). A major lung CD103 (alphaE)-beta7 integrin-positive epithelial dendritic cell population expressing Langerin and tight junction proteins. J. Immunol. *176*, 2161–2172.

Torosantucci, A., Bromuro, C., Chiani, P., De Bernardis, F., Berti, F., Galli, C., Norelli, F., Bellucci, C., Polonelli, L., Costantino, P., et al. (2005). A novel glyco-conjugate vaccine against fungal pathogens. J. Exp. Med. *202*, 597–606.

Torosantucci, A., Chiani, P., Bromuro, C., De Bernardis, F., Palma, A.S., Liu, Y., Mignogna, G., Maras, B., Colone, M., Stringaro, A., et al. (2009). Protection by anti-beta-glucan antibodies is associated with restricted beta-1,3 glucan binding specificity and inhibition of fungal growth and adherence. PLoS ONE *4*, e5392.

Traynor, T.R., Kuziel, W.A., Toews, G.B., and Huffnagle, G.B. (2000). CCR2 expression determines T1 versus T2 polarization during pulmonary Cryptococcus neoformans infection. J. Immunol. *164*, 2021–2027.

Waskow, C., Liu, K., Darrasse-Jeze, G., Guermonprez, P., Ginhoux, F., Merad, M., Shengelia, T., Yao, K., and Nussenzweig, M. (2008). The receptor tyrosine kinase Flt3 is required for dendritic cell development in peripheral lymphoid tissues. Nat. Immunol. *9*, 676–683.

Wolf, A.J., Linas, B., Trevejo-Nunez, G.J., Kincaid, E., Tamura, T., Takatsu, K., and Ernst, J.D. (2007). Mycobacterium tuberculosis infects dendritic cells with high frequency and impairs their function in vivo. J. Immunol. *179*, 2509–2519.